

Interpenetrated Metal–Organic Framework with Selective Gas Adsorption and Luminescent Properties

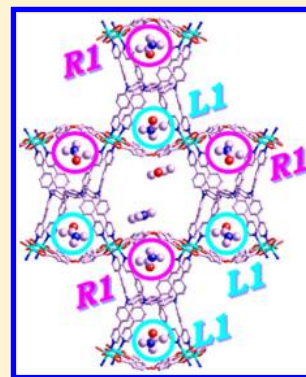
Ling Qin,[†] Ze-Min Ju,[†] Zhong-Jie Wang,[‡] Fan-Dian Meng,[†] He-Gen Zheng,^{*,†} and Jin-Xi Chen^{*,‡}

[†]State Key Laboratory of Coordination Chemistry, School of Chemistry and Chemical Engineering, Nanjing National Laboratory of Microstructures, Nanjing University, Nanjing 210093, PR China

[‡]School of Chemistry and Chemical Engineering, Southeast University, Nanjing 211189, PR China

S Supporting Information

ABSTRACT: A new 2-fold interpenetrated cadmium metal–organic framework $\{[\text{Cd}_2(\text{TPPBDA})(\text{OBA})_2]\cdot 4\text{DMA}\cdot 8\text{H}_2\text{O}\}_n$ (**1**) (Cd-MOF) (TPPBDA = *N,N,N',N'*-tetrakis(4-(4-pyridine)-phenyl)biphenyl-4,4'-diamine, H_2OBA = 4,4'-oxybis(benzoate), and DMA = *N,N*-dimethylacetamide) was synthesized by a solvothermal reaction. Compound **1** is a 3D net with a meso-helical chain. A noticeable structural feature is that the arrangement of lattice DMA molecules is different in the different meso-helical channels. The material exhibits gas sorption properties for CO_2 , H_2 , and CH_4 . The adsorption selectivity of CO_2/CH_4 was calculated from the single-component isotherms using the dual-site Langmuir–Freundlich-based ideal adsorbed solution theory. In addition, the luminescent properties of the Cd-MOF in the solid state and in suspension in different organic solvents was investigated.



■ INTRODUCTION

Metal–organic frameworks (MOFs) have attracted tremendous attention because of their ability to adjust their porosity and because of the functionalities that are incorporated in the frameworks.¹ As a result, numerous MOFs have been designed and synthesized for potential applications including gas storage and separation, nonlinear optics, magnetics, and catalysis.² Some properties, for example, gas sorption separation, depend mainly on pore size and shape, which is known as the molecular sieving effect.³ Zhou and co-workers reported an interpenetrated and porous net, PCN-17.⁴ The interpenetration and sulfate bridging in PCN-17 reduce its pore size to approximately 3.5 Å, leading to selective adsorption of H_2 and O_2 over N_2 and CO . Therefore, this material can be used for the separation of N_2 and O_2 , H_2 and CO , and N_2 and H_2 .⁴ However, some other properties may depend on the composition of the MOFs, such as sensing.⁵ For example, our group reported a rare nanotubular MOF that was constructed from the ligand 3,6-di(pyridin-4-yl)-1,2,4,5-tetrazine, in which the tetrazine ring plays the role of chromophore and exhibits a solvatochromic response to different solvent guest molecules.⁶ Thus, more and extensive efforts have been devoted to synthesizing porous MOFs because of their potential applications.

Many Cd-based MOFs have been reported in the literature;⁷ herein, we describe a new 2-fold interpenetrated framework $\{[\text{Cd}_2(\text{TPPBDA})(\text{OBA})_2]\cdot 4\text{DMA}\cdot 8\text{H}_2\text{O}\}_n$ (**1**) based on Cd(II), tetratopic pyridyl ligand *N,N,N',N'*-tetrakis(4-(4-pyridine)-phenyl)biphenyl-4,4'-diamine (TPPBDA), and a bent carboxylate ligand (H_2OBA = 4,4'-oxybis(benzoate)),⁸ DMA = *N,N*-dimethylacetamide). The crystal structure,

topological analysis, absorption performance and photoluminescent properties are studied in detail. The X-ray structure reveals that compound **1** is a doubly interpenetrated 3D network.

■ EXPERIMENTAL SECTION

General Methods. All chemicals and solvents used in the syntheses were of reagent grade and used without further purification. H_2OBA was used as commercially available. The TPPBDA ligand was prepared as follows on the basis of palladium-catalyzed cross-coupling reaction.

Preparation of *N,N,N',N'*-Tetrakis(4-bromophenyl)biphenyl-4,4'-diamine. An oven-dried 500 mL Schlenk flask was charged with tris(4-bromophenyl)amine (24.1 g, 50 mmol), and then ether (350 mL) and *N,N,N',N'*-tetramethylethylenediamine (8.2 mL) were added through a rubber septum. The reaction mixture was cooled to -78 °C. Upon slow addition of a *n*-BuLi solution (34 mL, 1.6 M in hexanes, 55 mmol), the mixture was stirred for 1 h at -78 °C. Solid CuCl_2 (10.8 g, 80 mmol) was added, and the reaction mixture was then allowed to warm slowly to room temperature and stirred for an additional 10 h. The reaction mixture was exposed to air, stirred for 30 min, and concentrated in vacuo. Chloroform (100 mL) and water (100 mL) were added, and the layers were separated. The aqueous layer was subsequently washed with chloroform (50 mL) three times. The organic extracts were combined, dried with MgSO_4 , and filtered. The volatile chloroform was removed under vacuum to leave a green solid. Purification by column chromatography (petroleum ether) yielded the pure product as a white solid (10.1 g, 50%). ¹H NMR ($\text{DMSO}-d_6$, 500 MHz, 25 °C): 7.61 (d, 4H), 7.5 (d, 8H), 7.09 (d, 4H), 7.0 (d, 8H).

Received: December 10, 2013

Revised: April 25, 2014

Published: April 30, 2014

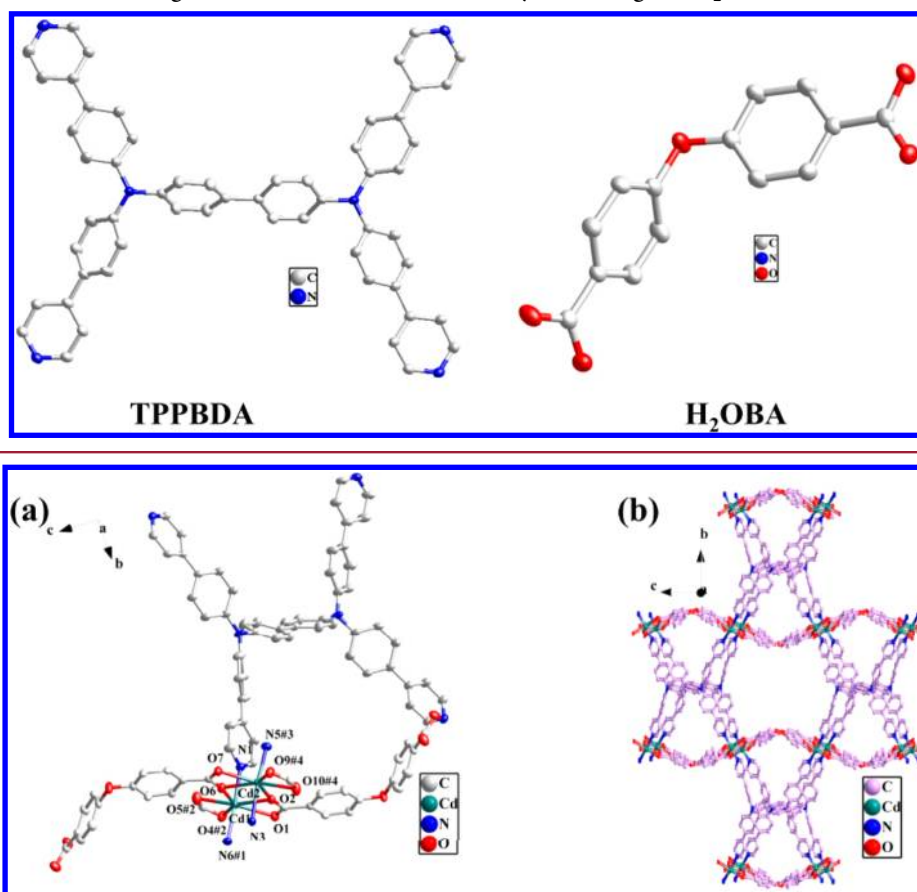
Scheme 1. Neutral Tetradentate Ligand TPPBDA and Bent Carboxylate Co-ligand H₂OBA

Figure 1. Coordination environment of the Cd(II) ions in **1** (hydrogen atoms and uncoordinated DMA and water molecules are omitted for clarity; 30% ellipsoid probability); symmetry codes: no. 1 = $-1/2 + x, 1/2 - y, 1/2 + z$; no. 2 = $1/2 + x, 1/2 - y, 1/2 + z$; no. 3 = $1 - x, -y, -z$; and no. 4 = $-1/2 + x, 1/2 - y, -1/2 + z$. (b) View of 3D framework of **1** along the *a* axis.

Preparation of *N,N,N',N'*-Tetrakis(4-(4-pyridine)-phenyl)-biphenyl-4,4'-diamine (TPPBDA). A 500 mL Schlenk flask was evacuated, backfilled with nitrogen, and charged with *N,N,N',N'*-tetrakis(4-bromophenyl)biphenyl-4,4'-diamine (8 g, 10 mmol), pyridine-4-boronic acid (8.41 g, 70 mmol), and K₂CO₃ (9.66 mg, 70 mmol). The flask was evacuated and backfilled with nitrogen, and Pd(PPh₃)₄ (2.2 mg, 0.05 mmol, 5.0 mol %) and 1,4-dioxane/H₂O (v/v = 3:2) were then added through a rubber septum. The reaction mixture was heated at 95 °C with stirring until the starting *N,N,N',N'*-tetrakis(4-bromophenyl)biphenyl-4,4'-diamine was completely consumed, as determined by TLC. The reaction mixture was then cooled to room temperature, and 1,4-dioxane was removed under vacuum. The aqueous mixture was extracted with chloroform (50 mL). The combined organic layers were dried over anhydrous MgSO₄, filtered, and concentrated in vacuo. The crude material was purified by chromatography on silica gel (ethyl acetate/methanol = 10:1), yielding the pure product as a yellow solid (4.2 g, 53%). ¹H NMR (DMSO-*d*₆, 500 MHz, 25 °C): 8.60 (s, 8H), 7.80 (d, 8H), 7.68 (s, 12H), 7.19 (d, 12H). ¹³C NMR (DMSO-*d*₆): 119.42, 120.41, 121.04, 124.33, 125.63, 128.15, 128.53, 131.85, 135.50, 145.91, 146.65, 148.12, 150.67. MS (ESI-TOF): calcd for C₃₆H₄₀N₆, 796; found, 797.

Synthesis of Complex 1. Compound **1** was synthesized by dissolving 39.8 mg of TPPBDA and 25.8 mg of H₂OBA in DMA (3 mL). A solution of 0.1 mmol aqueous Cd(NO₃)₂ was then added, and the mixture was placed in a Teflon vessel within an autoclave and heated at 85 °C for 3 days. Pale yellow prismatic crystals were obtained, filtered off, and dried under ambient conditions. The yield of the reaction was ca. 50% based on the TPPBDA ligand. Anal Calcd. for C₁₀₀H₁₀₈Cd₂N₁₀O₂₂: C, 59.62; H, 5.37; N, 6.91. Found: C, 59.24; H,

5.39; N, 6.88. The IR spectra of the corresponding complex is shown in Supporting Information Figure S8.

RESULTS AND DISCUSSION

Crystal Structure of {[Cd₂(TPPBDA)(OBA)₂]·4DMA·8H₂O}_n (1**).** Compound **1** crystallizes in the monoclinic crystal system with two Cd cations in the asymmetric unit (Figure 1a). (Crystal data and structure refinement parameters of compound **1** are given in Table 1.) Each Cd(II) unit has a [CdN₂O₅] coordination geometry. The OBA²⁻ ligand takes bidentate-chelation and μ₃-chelating-bridging tridentate coordination modes; two Cd(II) ions are bridged by two carboxylate O atoms, forming a four-membered square-shaped [Cd₂(CO₂)₄] ring. The OBA²⁻ anions connect to the [Cd₂(CO₂)₄] units to form 1D chains. Then, the chains are linked by the neutral tetradentate ligand to generate a 3D net (Figure 1b). It is worth noting that different shapes of channels are generated on the *ab*, *bc*, and *ac* planes in the individual network, as shown in Supporting Information Figure S1.

Compound **1** is a 3D net composed of meso-helical chains with a long pitch of 21.115 Å, which are labeled as the L1 and R1 chains (Figure 2a). The two symmetrically related helices coexist in the centrosymmetric solid, in which they appear in the left-handed and right-handed enantiomorphs, respectively. However, the L1- and R1-type single meso-helical chains are arranged alternatively, which indicates achirality and is further confirmed by the achiral space group, C₂/c. The central axis

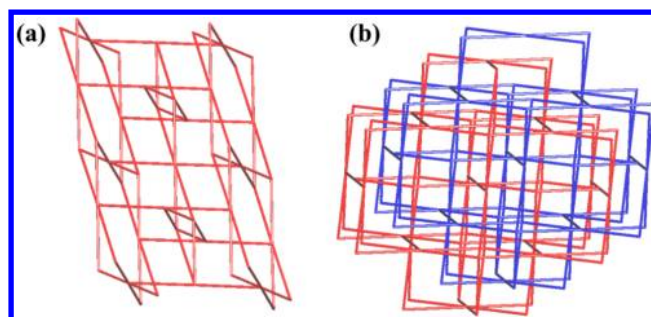
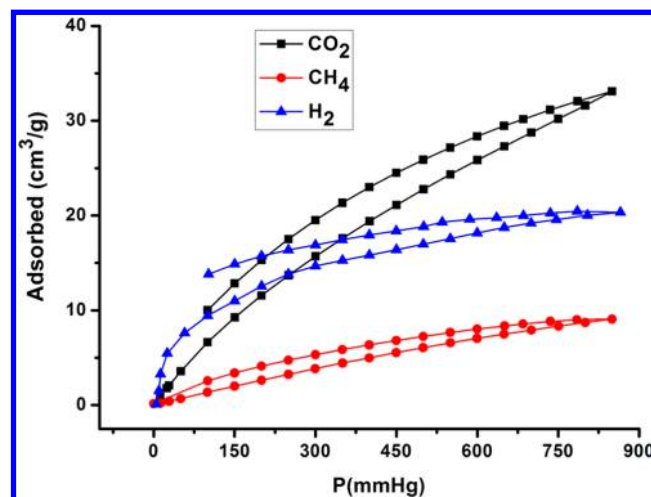
Table 1. Crystal Data and Structure Refinement Parameters of Compound 1

compound	1 ^c
empirical formula	C ₉₂ H ₇₄ Cd ₂ N ₈ O ₁₂
formula weight	1708.39
crystal system	monoclinic
space group	C2/c
a (Å)	21.1146(11)
b (Å)	37.6435(19)
c (Å)	28.2514(14)
α (deg)	90
β (deg)	108.8030(10)
γ (deg)	90
V (Å ³)	21256.6(19)
Z	8
D _{calcd} (g cm ⁻³)	1.068
μ (mm ⁻¹)	0.452
F(000)	6992
tot., uniq. data	59 725, 18 710
R(int)	0.0715
observed data [I > 2σ(I)]	10 839
N _{ref} , N _{par}	18 710, 1029
R ₁ ^a , wR ₂ ^b [I > 2σ(I)]	0.0391, 0.0820
GOF on F ²	1.035
min and max resd density (e Å ⁻³)	-0.391, 0.788

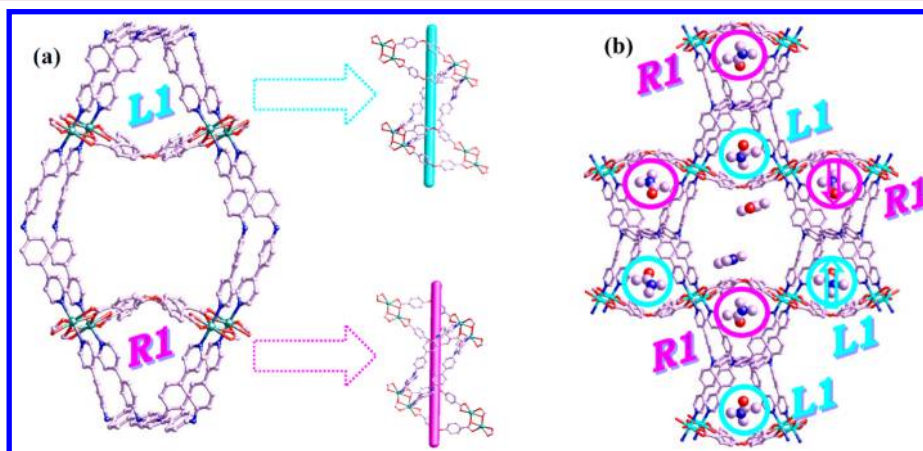
^aR₁ = Σ||F_o - F_c||/Σ|F_o|. ^bwR₂ = {Σ[w(F_o² - F_c²)²]/Σ[w(F_o²)²]}^{1/2}; where w = 1/[σ²(F_o²) + (aP)² + bP] and P = (F_o² + 2F_c²)/3. ^cThe residual electron densities were flattened by using the SQUEEZE option of PLATON.

about each helical chain is a 2-fold screw axis.⁹ The other structural feature is that the arrangement of lattice DMA molecules is different in the different meso-helical channels, which is attributed to the crystallographic symmetry. It can be seen that the O atoms of the DMA molecules are oriented upward in the L1 channels, whereas the O atoms are oriented downward in the R1 channels, as shown in Figure 2b.

Better insight into the nature of the intricate framework can be attained by the application of a topological approach,¹⁰ that is, reducing multidimensional structures to a simple node and connection net. As discussed above, [Cd₂(CO₂)₄] clusters are defined as 6-connected nodes. Likewise, TPPBDA ligands ligating with four [Cd₂(CO₂)₄] clusters can act as 4-connected

**Figure 3.** (a) Schematic representation of (4,6)-connected topology net. (b) Schematic view of the 2-fold interpenetrating framework.**Figure 4.** Gas adsorption isotherms for CO₂ (black) and CH₄ (red) at 273 K and for H₂ (blue) at 77 K.

nodes. On the basis of the simplification principle, the resulting structure is a (4,6)-connected net with point symbol {4⁶}-{4².6⁸.8⁸} (Figure 3a). The overall structure is a pair of identical nets, which are mutually interpenetrated to form a doubly interpenetrating framework (Figure 3b). Despite the framework interpenetration, the structure retains a 45.7% solvent-accessible void volume, as calculated by the PLATON program.¹¹ TGA reveals a 24% (by mass) loss of solvent, which is ascribed to the loss of four lattice DMA and eight water molecules, with a theoretical weight loss of 24.28%; the

**Figure 2.** (a) View of meso-helical chains (marked by L1 and R1) in net 1. (b) Perspective views of the different arrangement directions of guest DMA molecules, especially in the L1 and R1 channels. The hydrogen atoms and the squeezed guest molecules are omitted for clarity.

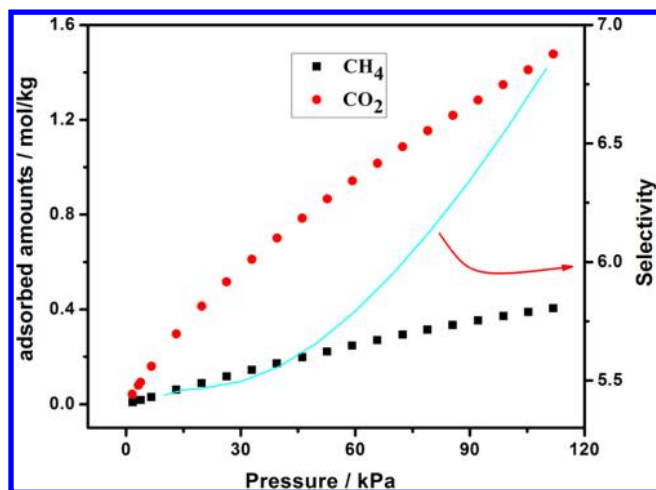


Figure 5. IAST-predicted isotherms and selectivity of equimolar mixtures of CO₂ and CH₄ in compound **1** at 298 K as a function of pressure.

decomposition of compound **1** starts at 350 °C (Supporting Information Figure S2).

Sorption Properties. With an increasing desire to use porous MOFs in storage applications, gas adsorptions for the Cd-MOF were measured. Adsorption measurements were performed on Micromeritics ASAP 2020 M+C surface area analyzer. Ultra-high-purity grade N₂, H₂, CO₂, and CH₄ (>99.999%) were used. All of the measured sorption isotherms were repeated twice to confirm reproducibility. Low-pressure H₂, CO₂, CH₄, and N₂ adsorption isotherms were measured at 273 and 298 K from 0 to 1 bar. There was little adsorption of N₂ up to 1 atm. The other adsorption data demonstrated that the compound selectively adsorbed CO₂ rather than CH₄ (Figure 4). This selective adsorption may be ascribed to the special quadrupole moment or the smaller gas molecule diameter of CO₂.¹² The CO₂ adsorption capacity for compound **1** at 273 and 298 K is shown in Supporting Information Figure S3. The isosteric heats of adsorption (Q_{st}) were calculated from the CO₂ adsorption isotherms using the Clausius–Clapeyron equation (for details, see the Supporting Information).¹³ A plot of the isosteric heat of adsorption (Q_{st}) as a function of CO₂ adsorbed quantity is shown in Supporting

Information Figure S4. The value of Q_{st} is about 23–25 kJ/mol, which is similar to the values for some other MOF materials.¹⁴

The selectivity of CO₂/CH₄ was calculated from the experimental single-component isotherms using the ideal adsorbed solution theory (IAST) method.¹⁵ The dual-site Langmuir–Freundlich equation was used to fit the experimental data.

$$q = q_{m1} \times \frac{b_1 \times p^{1/n_1}}{1 + b_1 \times p^{1/n_1}} + q_{m2} \times \frac{b_2 \times p^{1/n_2}}{1 + b_2 \times p^{1/n_2}}$$

The CO₂/CH₄ selectivity calculation was based on a CO₂/CH₄ mixture with CO₂/CH₄ = 1:1 at a total pressure of 1 atm. Adsorption isotherms predicted by IAST suggested that the dual-site Langmuir–Freundlich equation fit the single-component isotherms well, as shown in Figure 5. The r^2 (coefficient of determination) values for all of the fitted isotherms were 0.999995. For **1**, CO₂ is preferentially adsorbed over CH₄ because of the stronger interactions between CO₂ and the Cd-MOF.

Luminescent Properties and X-ray Powder Diffraction. Phase purity of the bulk material was confirmed by the comparison of its powder diffraction (PXRD) patterns with that simulated from single-crystal X-ray diffraction study (Supporting Information Figure S5). The solid-state emission spectrum for compound **1** exhibits a broad peak at 553 nm, which is more likely to be attributed to intraligand transition because an emission with a maximum at 558 nm is observed for TPPBDA (Supporting Information Figure S6). Some fluorescent MOF materials that are sensitive to guest solvent molecules have been reported.¹⁶ Motivated by previous works, the photoluminescent properties were also investigated in suspension in common solvents. A finely ground sample of compound **1** (10 mg) was immersed in different organic solvents (10 mL), treated by ultrasonication for 2 h, and then aged to form stable emulsions. The solvents tested were *N,N*-dimethylformamide (DMF), chloroform (CHCl₃), dichloromethane (CH₂Cl₂), acetonitrile (CH₃CN), and methanol (CH₃OH). As shown in Figure 6, the PL intensities are dependent on the solvent molecules, particularly in the case of DMF and CH₂Cl₂, which exhibit the most significant enhancing and quenching effects, respectively. In short, the intensities are affected by the solvents, with DMF > CH₃OH > CH₃CN > CHCl₃ > CH₂Cl₂ (Supporting Information Figure S7), which

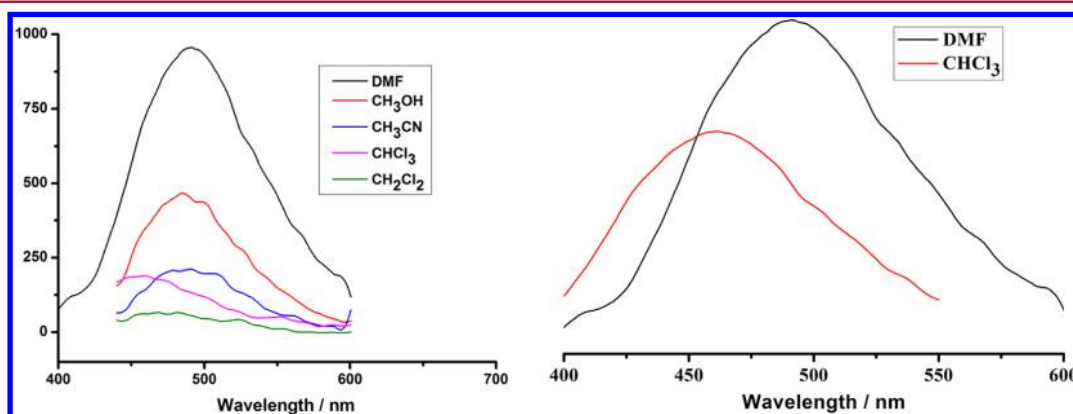


Figure 6. Left: emission of **1** suspended in various solvents (DMF, CH₃OH, CH₃CN, CHCl₃, and CH₂Cl₂) under the same testing conditions. Right: different emission peaks of **1** suspended in DMF or CHCl₃; the test conditions in CHCl₃ were further optimized to provide better data for comparison.

may be ascribed to the different solubility.¹⁷ The other interesting feature is that an emission with a maximum at 458 nm is observed in CHCl₃. However, the main emission peaks are centered at 495 nm in the other four solvents. The different emission peaks may be ascribed to specific host–guest recognition.¹⁸

CONCLUSIONS

We have successfully prepared a 3D porous network (Cd-MOF) based on TPPBDA and H₂OBA as coligands. The structure of the Cd-MOF is a doubly interpenetrated framework with a {4⁶}{4².6⁸.8⁵} net containing meso-helices. The Cd-MOF exhibits selective gas sorption for CO₂ over that of CH₄ and N₂. The selectivity of CO₂/CH₄ was calculated using the dual-site Langmuir–Freundlich-based ideal adsorbed solution theory method. Additionally, the luminescent properties of the Cd-MOF in the solid state and in suspension in different solvents were investigated.

ASSOCIATED CONTENT

Supporting Information

Crystallographic data in CIF format, selected bond lengths and angles, IR, TGA, PXRD, patterns of photochemistry, and gas adsorption data. This material is available free of charge via the Internet at <http://pubs.acs.org>.

AUTHOR INFORMATION

Corresponding Author

*(H.-G.Z.) E-mail: zhenghg@nju.edu.cn. Fax: 86-25-83314502.

Notes

The authors declare no competing financial interest.

ACKNOWLEDGMENTS

This work was supported by grants from the Natural Science Foundation of China (nos. 91022011, 21021062, 20971065, and 21371092) and the National Basic Research Program of China (no. 2010CB923303).

DEDICATION

Dedicated to Professor Xin-Quan Xin on the occasion of his 80th birthday.

REFERENCES

- (1) (a) Kong, X. Q.; Deng, H. X.; Yan, F. Y.; Kim, J.; Swisher, J. A.; Smit, B.; Yaghi, O. M.; Reimer, J. A. *Science* **2013**, *341*, 882. (b) Duan, J. G.; Higuchi, M.; Foo, M. L.; Horike, S.; Rao, K. P.; Kitagawa, S. *Inorg. Chem.* **2013**, *52*, 8244. (c) Deng, H. X.; Grunder, S.; Cordova, K. E.; Valente, C.; Furukawa, H.; Hmadeh, M.; Gándara, F.; Whalley, A. C.; Liu, Z.; Asahina, S.; Kazumori, H.; O’Keeffe, M.; Terasaki, O.; Stoddart, J. F.; Yaghi, O. M. *Science* **2012**, *336*, 1018.
- (2) (a) Wriedt, M.; Yakovenko, A. A.; Halder, G. J.; Prosvirin, A. V.; Dunbar, K. R.; Zhou, H. C. *J. Am. Chem. Soc.* **2013**, *135*, 4040. (b) Nugent, P.; Belmabkhout, Y.; Burd, S. D.; Cairns, A. J.; Luebke, R.; Forrest, K.; Pham, T.; Ma, S.; Space, B.; Wojtas, L.; Eddaoudi, M.; Zaworotko, M. J. *Nature* **2013**, *495*, 80. (c) Yang, Q. X.; Chen, Z. J.; Hu, J. S.; Hao, Y.; Li, Y. Z.; Lu, Q. Y.; Zheng, H. G. *Chem. Commun.* **2013**, *49*, 3585. (d) Wang, C.; Wang, J. L.; Lin, W. B. *J. Am. Chem. Soc.* **2012**, *134*, 19895.
- (3) (a) Fairen-Jimenez, D.; Moggach, S. A.; Wharmby, M. T.; Wright, P. A.; Parsons, S.; Düren, T. *J. Am. Chem. Soc.* **2011**, *133*, 8900. (b) Ma, S. Q.; Sun, D. F.; Yuan, D. Q.; Wang, X. S.; Zhou, H. C. *J. Am. Chem. Soc.* **2009**, *131*, 6445.
- (4) Ma, S. Q.; Yuan, D. Q.; Wang, X. S.; Zhou, H. C. *Inorg. Chem.* **2009**, *48*, 2072.

- (5) (a) Kreno, L. E.; Leong, K.; Farha, O. K.; Allendorf, M.; Van Duyne, R. P.; Hupp, J. T. *Chem. Rev.* **2012**, *112*, 1105. (b) Lu, G.; Hupp, J. T. *J. Am. Chem. Soc.* **2010**, *132*, 7832.
- (6) (a) Lu, Z. Z.; Zhang, R.; Pan, Z. R.; Li, Y. Z.; Guo, Z. J.; Zheng, H. G. *Chem.—Eur. J.* **2012**, *18*, 2812. (b) Lu, Z. Z.; Zhang, R.; Li, Y. Z.; Guo, Z. J.; Zheng, H. G. *J. Am. Chem. Soc.* **2011**, *133*, 4172.
- (7) (a) Sun, L.; Xing, H.; Xu, J.; Liang, Z.; Yu, J.; Xu, R. *Dalton Trans.* **2013**, *42*, 5508. (b) Li, C. P.; Du, M. *Inorg. Chem. Commun.* **2011**, *14*, 502. (c) Zheng, S. L.; Chen, X. M. *Aust. J. Chem.* **2004**, *57*, 703.
- (8) (a) Qin, L.; Hu, J. S.; Zhang, M. D.; Guo, Z. J.; Zheng, H. G. *Chem. Commun.* **2012**, *48*, 10757. (b) Mahata, P.; Sundaresan, A.; Natarajan, S. *Chem. Commun.* **2007**, *43*, 4471. (c) Wang, X. L.; Qin, C.; Wang, E. B.; Li, Y. G.; Su, Z. M.; Xu, L.; Carlucci, L. *Angew. Chem., Int. Ed.* **2005**, *44*, 5824.
- (9) Xu, L.; Qin, C.; Wang, X. L.; Wei, Y. G.; Wang, E. B. *Inorg. Chem.* **2003**, *42*, 7342.
- (10) Blatov, V. A.; Shevchenko, A. P.; Serezhkin, V. N. *J. Appl. Crystallogr.* **2000**, *33*, 1193.
- (11) Spek, A. L. *Acta Crystallogr., Sect. A* **1990**, *46*, 194.
- (12) (a) Cui, J. H.; Li, Y. Z.; Guo, Z. J.; Zheng, H. G. *Chem. Commun.* **2013**, *49*, 555. (b) Xiang, S. C.; He, Y. B.; Zhang, Z. J.; Wu, H.; Zhou, W.; Krishna, R.; Chen, B. L. *Nat. Commun.* **2012**, *3*, 954. (c) Ortiz, G.; Brandès, S.; Rousselin, Y.; Guillard, R. *Chem.—Eur. J.* **2011**, *17*, 6689.
- (13) (a) Si, X. L.; Jiao, C. L.; Li, F.; Zhang, J.; Wang, S.; Liu, S.; Li, Z. B.; Sun, L. X.; Xu, F.; Gabelicad, Z.; Schick, C. *Energy Environ. Sci.* **2011**, *4*, 4522. (b) Park, M.; Moon, D.; Yoon, J. W.; Chang, J. S.; Lah, M. S. *Chem. Commun.* **2009**, *45*, 2026.
- (14) (a) Llewellyn, P. L.; Bourrelly, S.; Serre, C.; Vimont, A.; Daturi, M.; Hamon, L.; Weireld, G. D.; Chang, J. S.; Hong, D. Y.; Hwang, Y. K.; Jhung, S. H.; Férey, G. *Langmuir* **2008**, *24*, 7245. (b) Loiseau, T.; Lecroq, L.; Volkringer, C.; Marrot, J.; Férey, G.; Haouas, M.; Taulelle, F.; Bourrelly, S.; Llewellyn, P. L.; Latroche, M. *J. Am. Chem. Soc.* **2006**, *128*, 10223. (c) Wang, Q. M.; Shen, D.; Bülow, M.; Lau, M. L.; Deng, S.; Fitch, F. R.; Lemcoff, N. O.; Semanscin, J. *Microporous Mesoporous Mater.* **2002**, *55*, 217.
- (15) (a) Karra, J. R.; Grabicka, B. E.; Huang, Y. G.; Walton, K. S. *J. Colloid Interface Sci.* **2013**, *392*, 331. (b) Peng, X.; Cheng, X.; Cao, D. P. *J. Mater. Chem.* **2011**, *21*, 11259. (c) Bae, Y. S.; Mulfort, K. L.; Frost, H.; Ryan, P.; Punnathanam, S.; Broadbelt, L. J.; Hupp, J. T.; Snurr, R. Q. *Langmuir* **2008**, *24*, 8592.
- (16) (a) Sun, C. Y.; Wang, X. L.; Qin, C.; Jin, J. L.; Su, Z. M.; Huang, P.; Shao, K. Z. *Chem.—Eur. J.* **2013**, *19*, 3639. (b) Cui, J. H.; Lu, Z. Z.; Li, Y. Z.; Guo, Z. J.; Zheng, H. G. *Chem. Commun.* **2012**, *48*, 7967. (c) Wang, C.; Lin, W. B. *J. Am. Chem. Soc.* **2011**, *133*, 4232. (d) Bauer, C. A.; Timofeeva, T. V.; Setterstten, T. B.; Patterson, B. D.; Liu, V. H.; Simmons, B. A.; Allendorf, M. D. *J. Am. Chem. Soc.* **2007**, *129*, 7136.
- (17) Song, J.; Zhou, Z.; Dong, X.; Huang, H.; Cao, D.; Liang, L.; Wang, K.; Zhang, J.; Chen, F. X.; Wu, Y. *J. Mater. Chem.* **2012**, *22*, 3201.
- (18) (a) Xie, Z.; Ma, L.; DeKrafft, K. E.; Jin, A.; Lin, W. *J. Am. Chem. Soc.* **2010**, *132*, 922. (b) Lan, A.; Li, K.; Wu, H.; Olson, D. H.; Emge, T. J.; Ki, W.; Hong, M.; Li, J. *Angew. Chem., Int. Ed.* **2009**, *48*, 2334. (c) Cui, J. H.; Lu, Z. Z.; Li, Y. Z.; Guo, Z. J.; Zheng, H. G. *Chem. Commun.* **2012**, *48*, 7967. (d) Wang, J. H.; Li, M.; Li, D. *Chem. Sci.* **2013**, *4*, 1793. (e) Dang, S.; Min, X.; Yang, W.; Yi, F. Y.; You, H.; Sun, Z. M. *Chem.—Eur. J.* **2013**, *19*, 17172.